

## Biomicrofluidic lab-on-chip device for cancer cell detection

J. H. He,<sup>1,a)</sup> J. Reboud,<sup>1</sup> H. Ji,<sup>1</sup> L. Zhang,<sup>1</sup> Y. Long,<sup>2</sup> and C. Lee<sup>1,3</sup>

<sup>1</sup>*Institute of Microelectronics, A\*STAR (Agency for Science, Technology and Research), 11 Science Park Road, Singapore 117685, Singapore*

<sup>2</sup>*School of Materials Science and Engineering, Nanyang Technological University, Nanyang Avenue, Singapore 639798, Singapore*

<sup>3</sup>*Department of Electrical and Computer Engineering, National University of Singapore, 4 Engineering Drive 3, Singapore 117576, Singapore*

(Received 1 September 2008; accepted 6 November 2008; published online 3 December 2008)

A lab-on-a-chip microfluidic device was designed, fabricated, and tested to be used in cancer cell or disease cell detection in body fluids. Mixtures of breast cancer cells MCF-7 and control cells MCF-10A were captured by meandering weir filters in microfluidic channels. A selective fluorescent complex 17 $\beta$ -estradiol-bovine serum albumin-fluorescein isothiocyanate enabled to specifically detect MCF-7 after only 4 min of contact. These signals are about seven times stronger than that of a labeling performed on conventional glass slides following the same protocol. The simple method could have the potential to replace complex existing cancer or disease detection schemes. © 2008 American Institute of Physics. [DOI: 10.1063/1.3040313]

Breast cancer is one of the most common diseases in women.<sup>1</sup> However, current clinical diagnostic approaches, for example, palpation, mammography, or needle biopsy,<sup>2</sup> do not sense abnormal cells until they become cancerous and invade nearby tissues. We propose a microfluidics lab-on-chip (LOC) device for cancer cell detection for potential application in early cancer diagnostics.

LOC devices can be used to study nucleic acids,<sup>3</sup> proteins, or cells.<sup>4</sup> In cell detection, the cells of interest are captured and then specifically identified as the targeted cells. For example, microfluidic channels with antibody-coated surfaces have been used to bind cervical cancer cells.<sup>5</sup> Another method<sup>6</sup> used magnetic fields to capture cells by trapping magnetic beads, coated with antibody probes that specifically bind to the cells. Furthermore, dielectrophoresis and laser light were used to confine the movement of microparticles and capture them.<sup>7</sup> These approaches require either additional chemical treatment on the surface of the microfluidic devices or beads, or an additional complicated experimental setup. In this study, we present a fast, straightforward, and sensitive approach for breast cancer cell detection. Both cancer cells and control cells are pumped into the LOC and captured by microweir filters. The cancer cells are detected by a fluorescent marker that selectively binds to specific receptors. The ligand estradiol (E2) is an estrogen, one of the predominant circulating ovarian steroid and the most biologically active hormone in the breast tissue. It is part of the fluorescent E2-bovine serum albumin-fluorescein isothiocyanate (E2-BSA-FITC) macromolecular complex used in this study.<sup>8</sup> E2 binds to specific estrogen receptors, which are known to be expressed in MCF-7 cells, whereas MCF-10A cells are negative.<sup>9</sup> They are found in the nucleus and the cytosol, and the complex E2-BSA-FITC has been used to identify more specifically those localized in the membrane of cells.<sup>10</sup>

Figure 1 shows the top view (a) and cross section (b) of the microfluidic device. It is comprised of one inlet, one outlet, and three chambers separated by two sets of filters

with a channel depth of 50  $\mu\text{m}$ . The first set of filters was made of pillars and was used to block unwanted big particles from going into the meandering trapping chamber (second chamber). The width and length of the rain-drop pillars were 45 and 90  $\mu\text{m}$ , respectively, while the spacing between the pillars was 30  $\mu\text{m}$ . The second set of filters consisted of meandering weir structures with a gap of 8  $\mu\text{m}$  between the Si weirs and the glass cover, for cell or bead capture. To optimize the cell capture, meandering structures increased the capture area and lowered the fluidic resistance, as compared to a straight-line weir filter.

The LOC fabrication started with two-mask UV lithography, and a two-step deep reactive ion etching defined the patterns of the channels using an oxide hard mask in the first step, and the meandering patterns in the second step, which were 8  $\mu\text{m}$  shorter than the first set of pillars. The inlet and outlet were created by potassium hydroxide (KOH) wet etching from the back side of the silicon (Si) wafer, with the front side of the wafer protected. Lastly, the patterned and etched Si wafer was bonded with a Pyrex glass wafer as top cover using anodic bonding. This fabrication process was adapted and updated from a DNA purification chip.<sup>11</sup> The 8 in. Si-Pyrex bonded wafers (images not shown) were diced into LOC sizes of 12  $\times$  18 mm<sup>2</sup> for testing. Figure 2(a) shows the LOC device at hand.

A customized plastic holder was designed to mount the device as shown in Fig. 2(b). It enabled the injection of the fluid samples in microliter volumes. An automatic syringe pump (KDS100, KD Scientific, Boston, MA) was used to

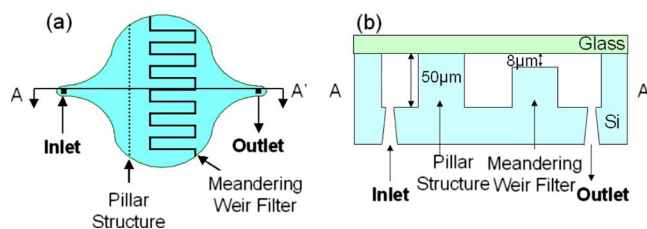


FIG. 1. (Color online) Schematic of the (a) top and (b) the cross section of the microfluidic device.

<sup>a)</sup>Electronic mail: han@ime.a-star.edu.sg.

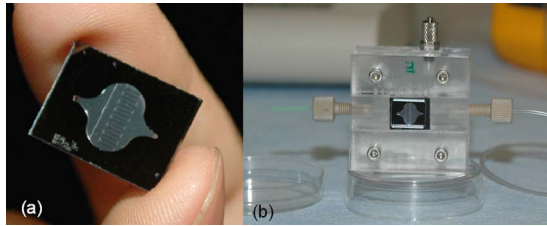


FIG. 2. (Color online) Image of the microfluidic device (a) at hand. (b) Inside the plastic testing holder.

inject step by step the washing buffers, the beads or the cell sample, and the dyeing solution into the inlet of the device. At the beginning of every experiment, phosphate buffer saline (PBS) was used to flush the device at a flow rate of  $50 \mu\text{l}/\text{min}$  for 2 min. PBS buffer was prepared and filtered through a  $0.45 \mu\text{m}$  membrane filter (Millipore, Cork, Ireland) prior to use.

To prove the capture capability of the device,  $10 \mu\text{m}$  diameter fluorescent beads (Molecular Probes, Inc., Eugene, OR) were used for flow tests. They were injected at the concentration of 1000 beads/ml and trapped in the second chamber at the meandering weirs. Figure 3(a) shows a  $45^\circ$  tilted scanning electron microscopy (SEM) image of a closer view of the captured bead, and Fig. 3(b) shows the cross section of the meandering weir and the captured bead after the glass cover is opened. These images indicate that our LOC devices can be used to trap and detect nondeformable objects that are bigger than the gap of the filter. Importantly, while scanning the weirs, it was found that the beads were captured near the glass cover in the majority of cases (results not shown). This position eases the focusing of optical systems and the detection, compared to devices capturing the cells in different planes, such as pillar-based chips.<sup>12</sup>

The same type of device was subsequently used to study the detection of MCF-7 and MCF-10A cells. Prior to injection in the device, approximately  $1 \times 10^6$  cells in 1 ml were dyed following standard labeling procedures. The nucleus of MCF-10A (noncancerous control cells) were dyed with Hoechst 33342 (Invitrogen, Inc. Carlsbad, CA) and showed in blue (emission peak at  $\sim 420 \text{ nm}$ ) in the fluorescent images, while MCF-7 cancer cells were dyed with Vybrant® DyeCycle™ Orange and showed in red ( $\sim 580 \text{ nm}$ ). The two cell lines were obtained from American Type Culture Collection (Manassas, VA) and cultured following the supplier's protocols. The diameters of MCF-7 and MCF-10A in suspension are similar, around  $15\text{--}20 \mu\text{m}$ .

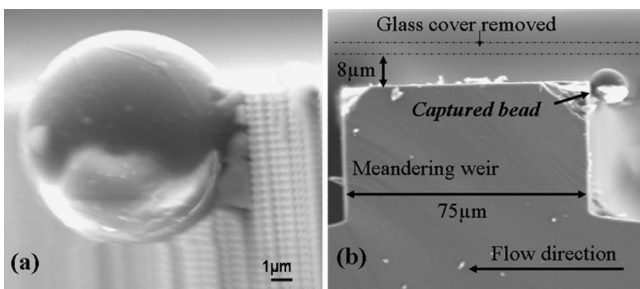


FIG. 3. SEM images of the meandering weirs after the glass cover is opened. (a)  $45^\circ$  view of the captured  $10 \mu\text{m}$  diameter polystyrene bead, (b) Cross section of the meandering weir and the captured bead.

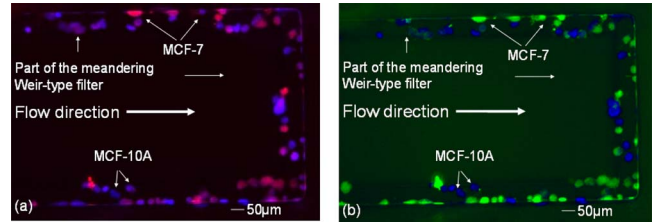


FIG. 4. (Color online) Overlap of two fluorescence images of the top view of the U-shaped meandering weirs. (a) MCF-10A were stained in blue by Hoechst, while MCF-7 were stained in red by Vybrant® DyeCycle™ Orange. (b) The label E2-BSA-FITC was introduced after capture and bound specifically to MCF-7 cells (not stained by Hoechst), shown in green here.

$500 \mu\text{l}$  of a mixture containing approximately 2000 dyed MCF-10A cells and 2000 dyed MCF-7 cells were injected into the device at a flow rate of  $50 \mu\text{l}/\text{min}$  and trapped by the meandering weirs. Figure 4(a) shows the overlap between two fluorescent images of the top view of the U-shaped meandering weirs that captured red MCF-7 cancer cells and blue MCF-10A control cells. This indicates the device capability to capture deformable objects: both breast cells, with diameters about twice as big as the gap, can be captured at the same time.

Immediately after that, the label  $0.1 \mu\text{M}$  E2-BSA-FITC (green, emission peak at about  $520 \text{ nm}$ , Sigma-Aldrich, St Louis, MO) in PBS was flushed through the device at a flow rate of  $20 \mu\text{l}/\text{min}$  for 1–7 min to selectively label the target cancer cell MCF-7. Finally, the device was washed with PBS ( $50 \mu\text{l}/\text{min}$  for 10 min). In both experiments, the captured cells were monitored by fluorescence imaging using an upright Olympus BX61 fluorescence microscope with an exposure of 100 ms with the software IMAGE-PRO 6.1 (Media Cybernetics, Bethesda, MD). The gray level images were artificially colored with the software to match the respective colors of the filters used.

Figure 4(b) is an overlap between two fluorescent images (using two filters, blue and green) of the top view of the U-shaped meandering weirs, showing the blue and green labels. By comparing Figs. 4(a) and 4(b), it was found that the cells in red in Fig. 4(a) were green in Fig. 4(b) and represented the cancer cell MCF-7 dyed by both Vybrant® DyeCycle™ Orange and E2-BSA-FITC, while the MCF-10A were blue but not green. This indicates that E2-BSA-FITC can be used as a specific marker for MCF-7 cancer cells and does not label MCF-10A noncancerous cells, in agreement with previous data.<sup>9</sup>

Labeling kinetics (Fig. 5) showed a better staining performance when compared to the standard use of glass slides, which is consistent with other reported microfluidic approaches. The green FITC fluorescence intensity signal was measured every minute for 7 min using the same exposure time of 100 ms. It was found that the green fluorescence signal (from 0 to 4096 for a 12 bit fluorescence image) increased from 1500 to 3500 in the first 4 min and entered into a plateau at 3500–3700. This may be due to the saturation of the binding sites on the cancer cell membrane by the FITC dye. A parallel test was conducted on a conventional glass slide, onto which  $10 \mu\text{l}$  of a suspension of cancer cells at the same concentration were deposited and incubated with a solution of  $0.1 \mu\text{M}$  E2-BSA-FITC for up to 7 min. At the fourth minute, it was found that the fluorescent signal from the LOC was about seven times stronger than when using a

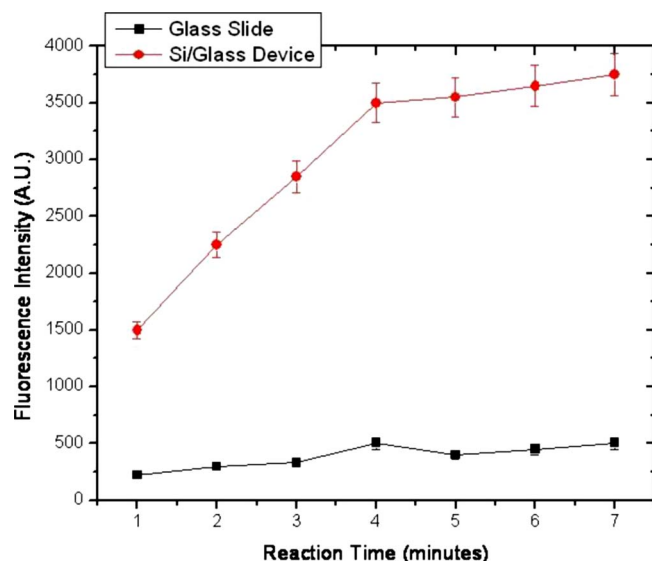


FIG. 5. (Color online) Fluorescence signal intensity (from 0 to 4096) against labeling reaction time (min) during staining of MCF-7 cancer cells with E2-BSA-FITC on a glass slide and under flow in the microfluidic device.

glass slide. The results strongly suggested that the microfluidic approach could achieve a much stronger signal for the same period of incubation. In other words, a microfluidic biochip could enable a much shorter detection time than conventional methods. This is probably due to the continuous flushing and refreshment of the labeling solution.

To conclude, body fluids or other fluid samples can be analyzed through the microfluidic cellular detection platform before the tumor grows into a detectable mass. This has great potential for early cancer and disease diagnostics as it ben-

efits from low sample volume, high sensitivity, and selectivity of the immunofluorescence approaches, as well as the rapid staining efficiency of microfluidic systems and manufacturability of the LOC by 8 in. wafer batch microfabrication process. This approach can be extended to the detection of other disease cells or pathogens.

This work was supported by the Science and Engineering Research Council of A\*STAR (Agency for Science, Technology, and Research), Singapore. Discussions with and help from S. Khon, S. Rafei, and K. Wang are acknowledged.

<sup>1</sup>M. A. Cuello, M. Nau, and S. Lipkowitz, *Breast Dis.* **15**, 71 (2002).

<sup>2</sup>F. Warnberg, H. Nordgren, L. Bergkvist, and L. Holmberg, *Br. J. Cancer* **85**, 869 (2001).

<sup>3</sup>W. C. Hui, L. Yobas, V. D. Samper, C. K. Heng, S. Liw, H. M. Ji, Y. Chen, C. Lin, J. Li, and T. M. Lim, *Sens. Actuators, A* **133**, 335 (2007).

<sup>4</sup>J. H. He, W. Xu, and L. Zhu, *Appl. Phys. Lett.* **90**, 023901 (2007).

<sup>5</sup>Z. Du, N. Colls, K. H. Cheng, M. W. Vaughn, and L. Gollahon, *Biosens. Bioelectron.* **21**, 1991 (2006).

<sup>6</sup>V. I. Furdul and D. J. Harrison, Proceedings of the MicroTAS, Monterey, CA, 2001 (unpublished).

<sup>7</sup>L. Luo, R. C. Salunga, H. Q. Guo, A. Bittner, K. C. Joy, J. E. Galindo, H. Xiao, K. E. Rogers, J. S. Wan, M. R. Jackson, and M. G. Erlander, *Nat. Med.* **5**, 117 (1999).

<sup>8</sup>J. Russo and I. H. Russo, *J. Steroid Biochem. Mol. Biol.* **102**, 89 (2006).

<sup>9</sup>A. Lostumbo, D. Mehta, S. Setty, and R. Nunezb, *Exp. Mol. Pathol.* **80**, 46 (2006).

<sup>10</sup>Y. Berthois, N. Pourreauschneider, P. Gandilhon, H. Mitre, N. Tubiana, and P. M. Martin, *J. Steroid Biochem. Mol. Biol.* **25**, 963 (1986).

<sup>11</sup>H. M. Ji, V. Samper, Y. Chen, W. C. Hui, H. J. Lye, F. Bte, A. C. L. Mustafa, L. Cong, C. K. Heng, and T. M. Lim, *Sens. Actuators, A* **139**, 139 (2007).

<sup>12</sup>H. Andersson, W. van der Wijngaart, P. Enoksson, and G. Stemme, *Sens. Actuators B* **67**, 203 (2000).